CHAPTER 8

Electron Transfer in Gaseous Positively Charged Peptides — Relation to Mass Spectrometry

Jack Simons

Contents

Abstract

Special theoretical tools are needed to carry out *ab initio* simulations of (i) electron transfer from a negatively charged donor (i.e., an anion donor) to a positively charged polypeptide and (ii) electron transfer within such a peptide from Rydberg orbitals on positive sites (e.g., protonated amines on side chains) to disulfide or amide bond sites. Basis sets capable of describing several Rydberg states as well as states with an electron attached to an SS σ^* or OCN π^* orbital must be used. Electron correlation is important to include for some states, and methods that allow one to obtain excited states of the same spin and spatial symmetry must be employed. Tools for treating surface hopping between states are also crucial. Examples of applying such tools to anion-to-peptide and intra-peptide electron-transfer processes are presented. It is demonstrated that intra-peptide electron transfer from Rydberg orbitals can occur over long distances (15 Å) and can take place in

Chemistry Department and Henry Eyring Center for Theoretical Chemistry, University of Utah, Salt Lake City, UT 84112, USA

Annual Reports in Computational Chemistry, Volume 5
ISSN: 1574-1400, DOI 10.1016/S1574-1400(09)00508-8

both through-space and through-bond paths. Similarities and differences with other electron-transfer processes in chemistry are also discussed.

Keywords: electron-capture dissociation; electron-transfer dissociation; electron transfer; Rydberg orbital; Landau–Zener theory

1. INTRODUCTION

Electron-capture dissociation (ECD) [1] and electron-transfer dissociation (ETD) [2] mass spectroscopic methods have shown much utility and promise for sequencing peptides and proteins. A strong point of both techniques is their propensity for selectively cleaving disulfide and N–C_α bonds and for doing so over a wide range of the backbone, thus producing many different fragment ions, unlike collision-induced dissociation (CID) or infrared multiphoton dissociation (IRMPD). ECD and ETD also preserve labile sidechains with posttranslational modifications. Parallel with many advances in the experimental development and improvement of these methods, theoretical studies have been carried out by several groups to try to determine the mechanism(s) [3] by which electron attachment leads to these specific bond cleavages as well as how the initial electron attachment occurs.

In both ECD and ETD experimental approaches, a positively charged sample of a polypeptide enters the gas phase (usually via electrospray), after which ions of specific mass to charge ratio are selected. Usually, the positive charging is induced by subjecting the solution-phase sample to acidic conditions prior to electrospray. An example of a relatively simple polypeptide is shown in Figure 1 as a means for introducing several concepts and terminology.

In ETD, an anion donor collides with the positively charged peptide and transfers an electron to the peptide; subsequent to this intermolecular electron transfer, the peptide undergoes cleavage at one of its N–C_α or S–S bonds to form fragment ions. The mass to charge ratios and intensities of the fragment ions are the raw data that is then used to infer the primary sequence of the original

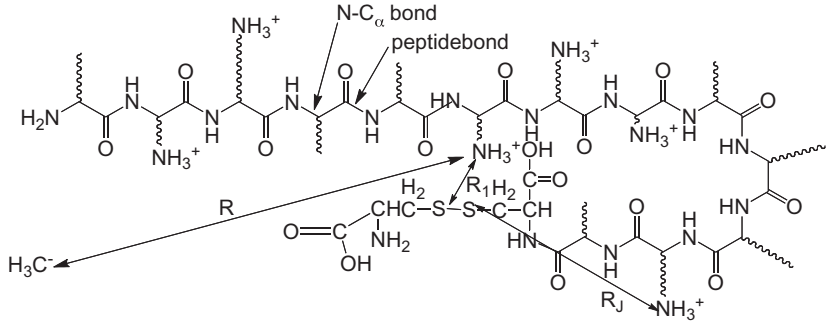

Figure 1 Prototypical polypeptide showing disulfide (SS) linkage, one of many N–C_α bonds, amino acid side chains (wavy lines), protonated amines on side chains (wavy lines), and one of many peptide bonds. Also shown is an anion donor (H_3C^-) colliding with the peptide.

polypeptide. In ECD, a free electron (usually having low kinetic energy) rather than a molecular anion collides with the parent polypeptide. This electron is captured and subsequently the peptide undergoes cleavage at one of its N–C_α or S–S bonds. The kind of fragment ions produced (i.e., those arising from N–C_α or S–S bond cleavage) and their intensities are found to be very similar for ETD and ECD, suggesting that the two processes proceed along very similar mechanistic paths. The detailed mechanism(s) by which the electron attaches to the peptide, where it attaches, and how the N–C_α or S–S bond cleavage then takes place have been the main focuses of our research in this area.

1.1 The electron-capture event involves electron transfer

In both ECD and ETD, the initial conditions appropriate to the experiments do not correspond to the ground electronic state of the electron/peptide (ECD) or anion/peptide (ETD) system. In both cases, there are a myriad of lower-energy electronic states, and this fact presents major challenges to the theoretical study of these processes. In Figure 2, we show qualitative plots of energies as functions of the distance R between a H_3C^- anion donor and a polypeptide having total charge Z.

The families of electronic states that must be considered in such a study and that are depicted in Figure 2 include:

1. The ion-pair state in which the "excess" electron resides on the donor anion; this state's energy varies strongly with R reflecting the strong Coulomb attraction between the anion donor and the positively charged polypeptide. In Figure 2, this state is shown as rapidly descending as R decreases approximately as expected based on the Coulomb attraction between the anion donor and the peptide of charge Z: $-14.4Z/R$ is in eV, when R is in Å.
2. Families of Rydberg states in which the excess electron has moved from the anion donor to reside in a Rydberg orbital (ground 3s, or excited 3p, 3d, 4s, etc.) on one of the polypeptide's protonated amine side chains. These curves (at least

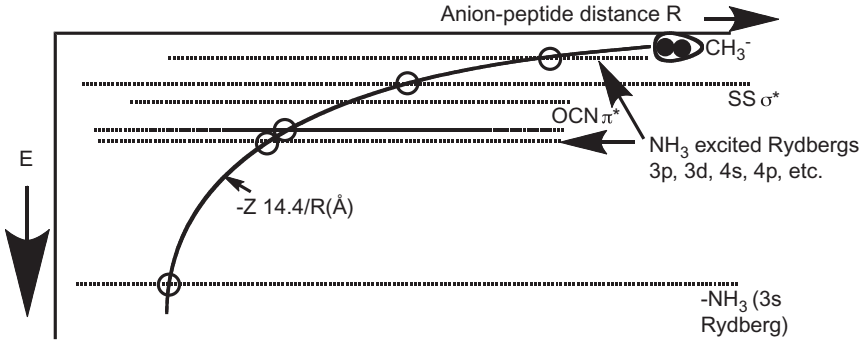

Figure 2 Qualitative plots of the electronic energy surfaces as functions of the anion-to-peptide distance R, for the anion–peptide collision complex, and for states in which the electron has been transferred from the anion to Rydberg states on one of the peptide's protonated amines, to an SS σ* orbital, or to an amide π* orbital.

at long anion–peptide distances) are found to vary rather weakly with R because the anion donor has been rendered neutral, so only charge–dipole and charge-induced-dipole potentials between the peptide and the H_3C radical exist.
3. One or more states in which the excess electron has moved to reside in an antibonding SS σ* orbital of one of the peptide's disulfide linkages.
4. One or more states in which the excess electron has moved to reside in an antibonding OCN π* orbital of one of the peptide's amide linkages. The curves of these σ* and π* vary rather weakly with R for the same reasons as noted above.

Near where we depict the energy surfaces crossing in Figure 2, the pairs of surfaces actually undergo avoided crossings at which they experience a minimum energy splitting that we denote $2H_{1,2}$. Moving through each such avoided crossing, the nature of the two states changes. For example, when the ion-pair state approaches the $-NH_3$ 3s ground-Rydberg state from above at the left-most circle in Figure 2, the lower-energy surface corresponds to having the extra electron in the 3s Rydberg orbital; the upper surface has this electron in the methyl lone pair orbital. In contrast, to the left of the circle, the lower surface corresponds to the ion-pair state, while the upper surface is the 3s Rydberg-attached state. The evolution of the two states' energies and wave functions through such avoided crossings describes how the interspecies electron transfer occurs. This is the *first category of electron-transfer processes* one needs to study when investigating ETD or ECD.

In probing ETD experiments, one must be able to characterize the above four families of electronic energy surfaces, and one must have a means of extracting the couplings $H_{1,2}$ between these states as they undergo avoided crossings. In the studies that our group has undertaken [3h–3w], we have used Landau–Zener (LZ) theory to estimate the probabilities P for an electron being transferred from an anion donor to a Rydberg orbital, an SS σ* orbital, or an amide π* orbital during a collision beginning on the attractive ion-pair surface that undergoes a crossing with one of the other surfaces. In LZ theory, this probability is computed as

$$P = 1 - \exp\left[-\frac{2\pi H_{1,2}^2}{\hbar v|\Delta F|}\right] \approx \frac{2\pi H_{1,2}^2}{\hbar v|\Delta F|} \tag{1}$$

$H_{1,2}$ is one half the splitting observed when the two energy surfaces undergo their avoided crossing, v the speed at which the łion pair moves through the avoided crossing region, and ΔF the difference in the slopes of the two energy surfaces as they approach the avoided crossing.

1.2 Intra-peptide electron transfer can also occur

Once an electron is transferred to or captured by the polypeptide, various things can happen:

1. If the electron attaches directly to an SS σ* orbital, the disulfide bond promptly cleaves [3j] because the $\sigma^2\sigma^{*1}$ electron-attached state is strongly

repulsive along the S–S bond. This is one path by which disulfide cleavage occurs.

2. If the electron enters an OCN π* orbital, an $^{-}$O–C•–NH–C_α radical anion center is formed, after which the neighboring N–C_α bond is weakened and can be cleaved (to produce $^{-}$O–C═NH + •C_α) thus producing the N–C_α bond-cleavage products [3m].
3. If the electron enters a Rydberg orbital on one of the protonated amine sites, in addition to undergoing a cascade of radiative or non-radiative relaxation steps to lower-energy Rydberg states, it can subsequently undergo intra-peptide electron transfer to either an SS σ* or an OCN π* orbital after which disulfide or N–C_α bond cleavage can occur [3r,3u–3w].

For the intra-peptide electron migration to be effective in cleaving an S–S or N–C_α bond, it must occur before the Rydberg species from which the electron is transferred can decay by some other mechanism. It is believed that electron attachment (in ECD or ETD) at a positively charged side chain initially occurs into an excited-Rydberg orbital after which a decay cascade eventually leads to formation of the ground-Rydberg species. It is known that excited-Rydberg states belonging to protonated or fixed-charge amine sites undergo radiationless relaxation to the ground-Rydberg state in a few to several microseconds. Moreover, we know that the excited-Rydberg states do not undergo N–H or N–C bond cleavage, but the ground-Rydberg states do (in *ca.* 10^{-12} s). Hence, the intra-peptide electron transfer must occur within a few microseconds of the time the electron attaches to an excited-Rydberg orbital; otherwise, it will relax to the ground-Rydberg state and N–H or N–C bond cleavage will occur (ejecting an H atom or an alkyl radical) terminating the electron's chance to undergo further transfer.

This transfer from a Rydberg orbital to an SS or OCN antibonding orbital is the *second family of electron-transfer events* that must be considered when studying ECD or ETD. These transfers can occur either through-space or through-bond. To appreciate which Rydberg states are most likely to be involved, qualitative depictions of the energies of states in which the extra electron occupies a Rydberg orbital or an SS σ* orbital are shown in Figure 3 as functions of the S–S bond length.

The energy profile of the SS σ*-attached state is largely repulsive,[1] but its location, relative to the parent and Rydberg-attached states, depends upon the distance *R* between the SS bond and the positively charged site whose Coulomb potential acts to move the SS σ*-attached state up and down in energy as *R* varies. For example, if *R* is very large, the energy of the SS σ*-attached state will be little affected by the stabilizing Coulomb potential of the $-NH_3^+$ site and thus its energy profile will be as shown by the upper curve in Figure 3. Alternatively, if the $-NH_3^+$ site is closer to the SS bond, the energy profile will be shifted downward as in the lower curve in Figure 3.

For each instantaneous value of the Coulomb potential experienced by the SS σ* orbital, a different Rydberg state will intersect the energy profile of the

[1]This state's energy is weakly attractive at large distances because of van der Waals and charge-induced dipole interactions, but its valence-range character is repulsive.

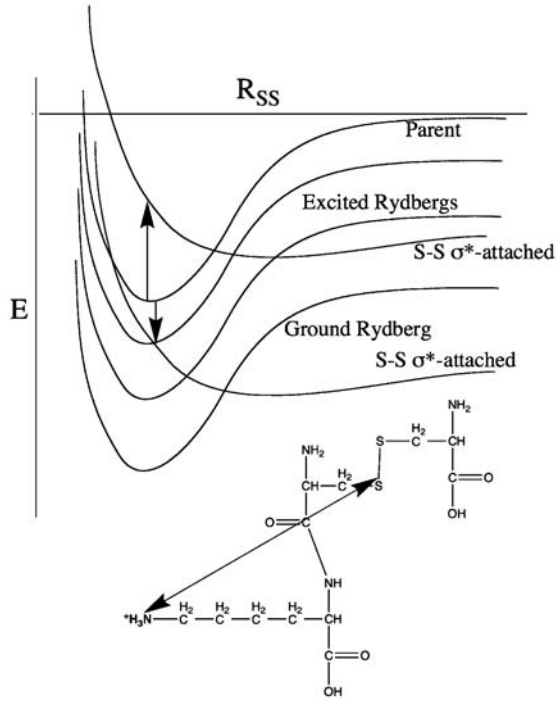

Figure 3 Energies, as functions of the S–S bond length, of the parent charged polypeptide (top), of ground and excited-Rydberg states localized on the protonated amine side chain, and of the SS σ*-attached state in the absence of (upper curve) and in the presence of (lower curve) Coulomb stabilization (appears as Figure 1 in ref. 3s).

SS σ*-attached state at or near the equilibrium SS bond length R_e. In polypeptides containing multiple positively charged sites such as that shown in Figure 4, the total Coulomb potential C

$$C = -14.4 \sum_J \frac{1}{R_J} \tag{2}$$

will determine the energy-placement of the SS σ*-attached state (R_J is the distance of the Jth charged site to the SS bond).

Because ETD and ECD experiments are carried out at or near room temperature, the SS and N–C_α bonds are expected to sample only distances close to their equilibrium values R_e. Hence, we focus primarily on the Rydberg states having energies close to that of the SS σ*-attached or OCN π*-attached state near R_e when considering intra-peptide electron transfer. In Figure 3, this would be the highest Rydberg state shown.

In the studies our group has undertaken [3h–3w] to date, we used LZ theory to estimate the probabilities P for an electron being transferred from such a Rydberg orbital to an SS σ* or amide π* orbital. In Figure 5 we show actual data from such a study on the $H_3C{-}S{-}S{-}(CH_2)_3{-}NH_3^+$ model compound.

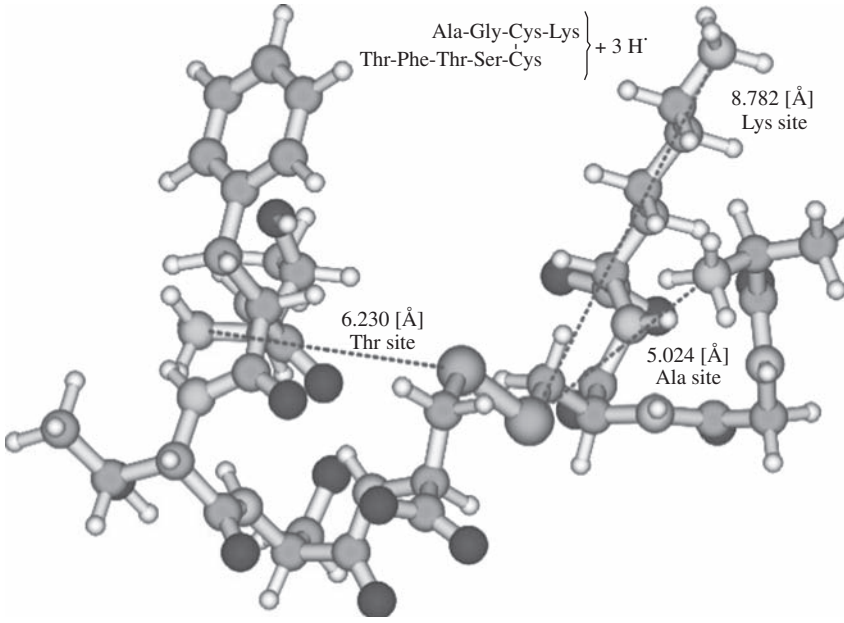

Figure 4 Triply protonated polypeptide containing one SS linkage with the distances R_j to each positive site labeled by dotted lines (appears in Figure 7 of ref. 3s).

From the data shown in Figure 5, we concluded that it is the excited-Rydberg state that crosses the repulsive SS σ*-attached state near R_e, so this is the state from which electron transfer is most likely to occur. The $82\,cm^{-1}$ energy value shown in Figure 5 is the electronic coupling matrix element $H_{1,2}$ connecting the excited-Rydberg and SS σ* states, which plays a central role in determining the LZ-estimated probability P of electron transfer (see Equation (1)). In these cases, the rates of electron transfer are computed by multiplying the frequency v at which the S–S bond moves through the curve crossing (we take this to be the harmonic frequency of the SS bond) by the LZ probability P. In the LZ formula, the speed v at which the system passes through the crossing region is computed in terms of the speed of the SS vibrational motion.

To illustrate, it was shown in ref. 3q that $H_{1,2}$ values in the $300\,cm^{-1}$ range produce LZ probabilities of *ca.* 0.1–0.5 for this system. Thus, we can estimate the rates of electron transfer by multiplying the S–S vibrational frequency v_{SS} (*ca.* $1.5 \times 10^{13}\,s^{-1}$) by the surface hopping probability (0.1–0.5) and then scaling by the ratio of the square of ($H_{1,2}/300$):

$$\text{Rate} \approx (1.5 \text{ to } 7.5) \times 10^{12} \left[\frac{H_{1,2}}{300}\right]^2 s^{-1} \tag{3}$$

Such estimates allowed us to conclude that the smallest $H_{1,2}$ that could produce S–S bond cleavage competitive with relaxation from one Rydberg state to another (taking place at *ca.* $10^6\,s^{-1}$) should be $H_{1,2}^{min} \approx 0.11 - 0.24\,cm^{-1}$. Most of the $H_{1,2}$ values we obtained in our studies to date are substantially larger,

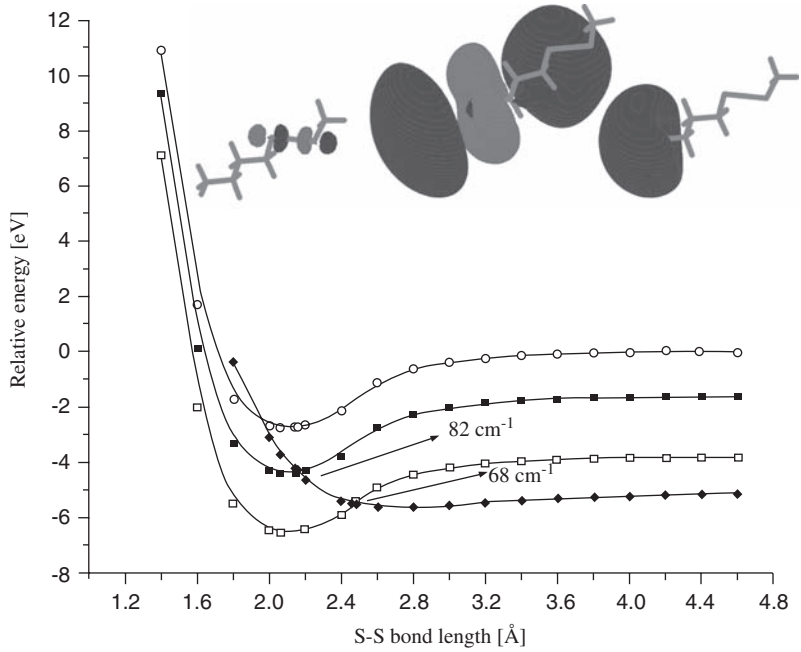

Figure 5 Energies of the parent $H_3C-S-S-(CH_2)_3-NH_3^+$ cation (open circles), ground Rydberg-attached (open squares), excited Rydberg-attached (filled squares), and S–S σ^*-attached (filed diamonds) states as functions of the S–S bond length. Also shown are the SS σ^* (left), excited-Rydberg (center), and ground-Rydberg (right) orbitals (appears as Figure 4 in ref. 3s).

suggesting that intra-peptide electron transfer can be an important contributor to electrons attaching to and cleaving SS and N–C_α bonds.

In summary, ETD and ECD processes involve two kinds of electron-transfer events. The first occurs in the initial capture of an electron by the positively charged polypeptide. The second involves intra-peptide electron transfer from a Rydberg orbital residing on a positively charged site to an SS or OCN bond site.

2. THE THEORETICAL CHALLENGES AND EXAMPLES OF HOW THE STUDIES ARE PERFORMED

2.1 Theoretical considerations

Before discussing specific examples as a tool for illustrating how one uses theory to carry out such studies, we overview a few components of all theoretical investigations of the electron-transfer events we have studied. Specifically, one must be sure to address all of the following issues:

1. Atomic orbital basis sets containing diffuse functions must be used at least for the atoms onto which the electron will attach. This means the sulfur atoms if one is studying disulfide cleavage and the O, C, and N atoms (at the site of cleavage) if one is studying N–C_α cleavage. It is important to then check to

make sure one obtains a reasonably accurate electron binding energy for the fragment that holds the excess electron upon bond cleavage. For SS bond cleavage, this means verifying that the $^{-}$S–R anion has an electron binding energy near 1.4 eV. This is important because the relative energies of the bond-attached and Rydberg-attached states determine which Rydberg state is likely to couple to the bond-attached state.

2. The positively charged site to which an electron is to attach must have special basis functions [4–6] attached to it to describe the Rydberg orbitals. This is important because one needs to accurately describe the energies of the Rydberg states in relation to bond-attached states and the Rydberg orbitals' radial extent must be properly represented. To appreciate the sizes of such orbitals, we show in Figure 6 the lowest (labeled 3s, 3p, 3d, 4s, 4p, and 5s because NH_4^+ is isoelectronic with Na^+) Rydberg orbitals of NH_4.

In each orbital, the outer surface in the figure contains only 60% of the electron density (i.e., 40% of the density lies farther from the cation center). Moreover, for each orbital, one can notice the size of the van der Waals surface of the underlying NH_4^+ cation to gain perspective about how large these Rydberg orbitals are. Realizing that the N–H bond length is *ca.* 1 Å, it is easy to appreciate that these Rydberg orbitals span (even at the 60% contour level) 10 Å or more.[2]

3. The theoretical methods used must be capable of describing not only ground but also (several) excited states, including state of the same spatial and spin symmetry. We have found it possible to converge Hartree–Fock self-consistent field (HF-SCF) calculations on excited states by starting the SCF process with a spin-orbital occupancy that describes the desired electronic state. After converging the SCF calculation and checking to make sure it has converged to the correct state, we have employed Møller–Plesset perturbation theory at second order (MP2) to evaluate the energy of each state. A correlated treatment is not so important for the Rydberg-attached states because they

[2]Hydrogenic and Rydberg orbitals have "sizes" that can be characterized by their expectation values of r and of r^2:

$$\langle r\rangle_{n,l} = \frac{n^2 a_0}{Z}\left[1.5 - \frac{l(l+1)}{2n^2}\right]; \quad \langle r^2\rangle_{n,l} = \frac{n^4 a_0^2}{Z^2}\left[2.5 - \frac{3l(l+1)-1}{2n^2}\right]$$

where n and l are the principal and angular momentum quantum numbers of the orbital and a_0 the Bohr unit of length ($a_0 = 0.529$ Å). These expressions can be found, for example, in ref. 7. To conceptualize the magnitude of the overlap (and thus the $H_{1,2}$ coupling strength) of a Rydberg orbital with, for example, a methyl anion lone pair, an SS σ*, or an amide π* orbital, think of a Rydberg s-orbital as a spherical shell of radius $\langle r\rangle_{n0} = 1.5n^2a_0/Z$ having a radial "thickness" δr to its electron distribution characterized by its dispersion in radial distribution $\delta r = [\langle r^2\rangle_{n,0} - (\langle r\rangle_{n,0})^2]^{1/2} = 0.5n^2a_0/Z$. This shell of thickness δr thus has a surface area of $4\pi 2.25n^4a_0^2/Z^2$ and a volume of $V_n = 4\pi 2.25 \times 0.5n^6a_0^3/Z^3$. In contrast, a methyl anion lone pair, an SS σ*, or an amide π* orbital has a volume of *ca.* $V_{\text{bond}} = 4/3\pi(10a_0)^3$. Now, consider one of the latter orbitals penetrating into a Rydberg orbital, and approximate the electron density within each of the two volumes V_n and V_{bond} as uniform. That is, within each volume, the respective wave functions are approximated by $\psi(\mathbf{r}) = (1/V)^{1/2}$. The $H_{1,2}$ coupling should then scale with n in the same manner as the overlap integral (S) between the two wave functions $S = \int_{V_{\text{bond}}}(1/V_{\text{bond}}^{1/2})(1/V_n^{1/2})d^3r = (V_{\text{bond}}^{1/2}/V_n^{1/2}) = \sqrt{10^3Z^3/0.5(3)(2.25)n^6}$ given in terms of the square root of the fraction of the volume of the Rydberg orbital that is shared with the penetrating orbital of volume $(10a_0)^3$. Even for $n = 4$, this overlap is $0.27Z^{2/3}$. For $n = 9$, S is $0.02Z^{3/2}$. This scaling of the overlap between a Rydberg orbital and a valence-sized orbital as n^{-3} suggests that the $H_{1,2}$ couplings will be small except for Rydberg orbitals in the $n = 3$–10 range, not for high-n Rydberg orbitals.

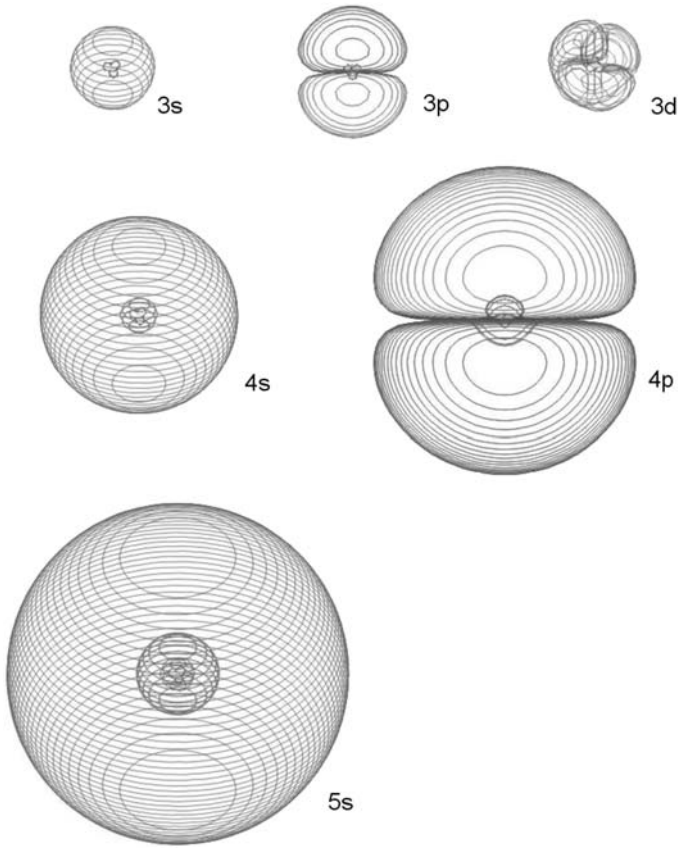

Figure 6 Plots of 3s, 3p, 3d, 4s, and 5s Rydberg orbitals of NH_4 with the outermost contour containing 60% of the electron density of that orbital.

have only one electron in their Rydberg orbital. However, for an anion donor such as H_3C^-, correlation is very important because the extra electron experiences very large correlations with the other methyl lone pair electron.

4. To evaluate the $H_{1,2}$ couplings, one needs to carry out calculations at a very finely spaced grid (often with geometry changes along, for example, the SS bond length, of *ca.* 0.01 Å) in the region of the avoided crossing. After one has determined the smallest energy gap between the two states undergoing the avoided crossing, $H_{1,2}$ is taken an one-half this gap. These same calculations are what one uses to evaluate the slope difference $|\Delta F|$ entering into the LZ surface hopping probability formula.

Finally, it is important to explain the strategy that we have used to construct model compounds on which to carry out *ab initio* calculations from which we can gain insight into the two classes of electron transfer discussed above. For the kind of polypeptides shown in Figures 1 and 4 and for most species used in ETD or ECD experiments, the positively charged sites reside primarily on side chains that possess great motional flexibility. This means that, as the peptide undergoes

thermal motion in the gas phase, the distances between the positive sites and any SS or OCN group will fluctuate substantially, as will the distances from one positive site to another. As a result, the Coulomb stabilization energy (Equation (2)) at the SS, OCN, and positive sites will also fluctuate with time. Ideally then, one would like to model the dynamical motions of the polypeptide's side chains and backbone and, at each instant of time, compute the rates for electron transfer from an anion donor to SS, OCN, and Rydberg sites as well as the rates of intra-peptide electron transfer. Such an ideal approach is simply not computationally feasible because of the substantial difficulties involved in each electron transfer rate calculation. Therefore, the approach we have undertaken involves:

a. Using small model compounds containing one disulfide or amide unit to limit the computational cost.
b. Fixing the distances between positive sites and SS or OCN bond sites and between positive sites in each calculation (but varying them from one calculation to another) as a way to gain data representative of that particular set of inter-site distances.

This approach allows us to generate a body of data representative of the range of geometries sampled by a polypeptide undergoing dynamical motions.

2.2 Illustrative examples

With the above advice and strategy in mind, we can now focus on a few illustrative cases involving electron transfer to an SS σ* orbital that subsequently affects disulfide bond cleavage as a means of further illustrating how these studies proceed and what they have told us. First, let us consider intra-peptide transfer from a Rydberg orbital on a protonated amine site, through intervening aliphatic ''spacers'' of varying length, to such an SS σ* orbital.

In Figure 7, we show the SS σ*, excited-Rydberg, and ground-Rydberg orbitals for three model compounds $^{+}H_3N–(CH_2)_n–S–S–CH_3$ having $n = 3$, 2, or 1 from left to right.

It is important to recognize that the Rydberg orbitals have significant amplitudes in regions of space where the SS σ* orbital also does and that the degree of overlap between the Rydberg and SS σ* orbitals decreases as n increases, as expected.

For $n = 3$, the energy profiles of the parent compound, the species with an electron attached to the ground or excited-Rydberg orbital, and the species with an electron in the SS σ* orbital as functions of the SS bond length were shown earlier in Figure 3 where we also see the $H_{1,2}$ values associated with the Rydberg SS σ* avoided crossings. Analogous data was obtained for the $n = 2$ and $n = 3$ cases, and the corresponding $H_{1,2}$ values were obtained. When the ln $H_{1,2}$ values for ground and excited-Rydberg states are plotted for $n = 1$, 2, and 3 are plotted vs. the distance R between the center of the SS bond and the center of charge of the Rydberg orbital, decent linear correlations are obtained as shown in Figure 8.

Such exponential decays of $H_{1,2}$ with distance are characteristic of the electronic coupling strengths in all electron-transfer studies [8–11], not just those

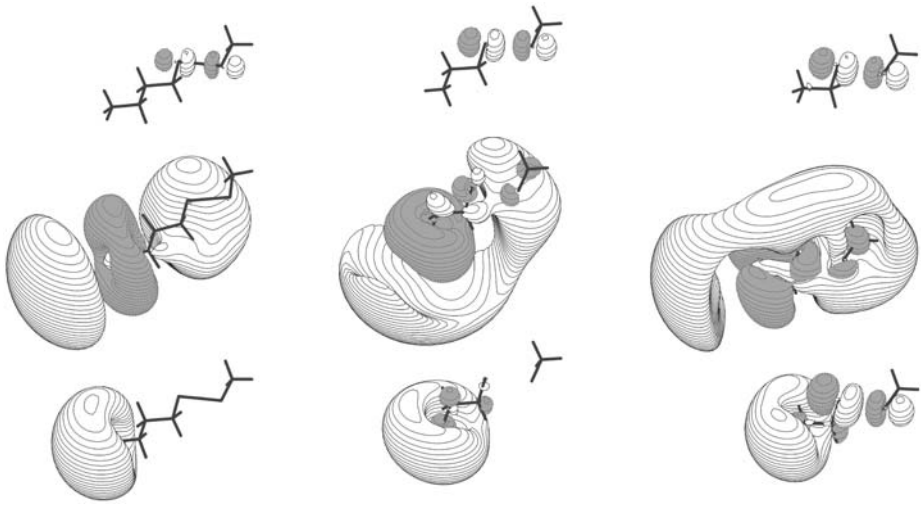

Figure 7 SS σ* (top), excited-Rydberg (middle), and ground-Rydberg (bottom) orbitals of $^{+}H_3N–(CH_2)_n–S–S–CH_3$ with $n = 3$ (left), 2 (center), and 1 (right) (appears as Figure 5 in ref. 3s).

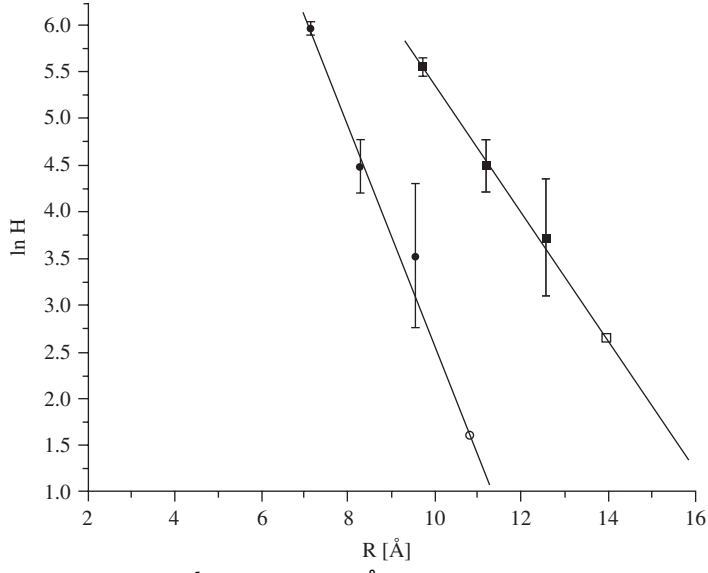

Figure 8 Plots of ln $H_{1,2}$ (cm^{-1}) vs. distance R (Å) from the center of the SS bond and the center of charge of the ground (left line) and excited (right line) Rydberg orbitals for the $^{+}H_3N–(CH_2)_n–S–S–CH_3$ model compounds having $n = 1$, 2, and 3 (appears as Figure 6 in ref. 3s).

related to intra-peptide or anion-to-peptide electron transfer. The error bars shown in Figure 8 derive from our estimate of how small $H_{1,2}$ can be before we find it too difficult to reliably determine the minimum energy splitting between two surfaces undergoing an avoided crossing.

Although we are not able to directly determine $H_{1,2}$ values as small as $0.3\,cm^{-1}$ (recall, this is the smallest $H_{1,2}$ that can generate an intra-peptide electron transfer that can compete with relaxations among Rydberg states), we use the near-linear plots of $H_{1,2}$ vs. R to extrapolate to that R-value where $H_{1,2}^{min} = 0.3\,cm^{-1}$ should be realized. For example, the data shown in Figure 8 suggest that the excited-Rydberg state can contribute to electron transfer out to $R \approx 18$ Å, while the ground-Rydberg state can out to $R \approx 12$ Å.

To explore whether the electron-transfer events occur primarily through-space or through-bond, we carried out calculations on model compounds in which the disulfide linkage is separated from the site of the Rydberg orbital(s) by distances similar to those arising in the studies of $^{+}H_3N–(CH_2)_n–S–S–CH_3$ but with no "spacer" groups between the Rydberg and SS sites. For example, we studied two model systems: $H_3C–SS–CH_3$ with an NH_4^+ ion 3–15 Å from the midpoint of the SS bond and $H_3C–SS–CH_3$ with an $N(CH_3)_4^+$ ion 3–15 Å from the midpoint of the SS bond. These two positive sites were chosen to model protonated amine and so-called fixed-charge sites that occur in many polypeptides. The energy profiles of the parent compound and of species with an electron attached to the SS σ*, ground-, or excited-Rydberg orbitals are shown in Figures 9 and 10.

Also shown in Figures 9 and 10 are the $H_{1,2}$ values (in cm^{-1}) obtained by analyzing the avoided curve crossings. In Figure 11 we show plots of the natural

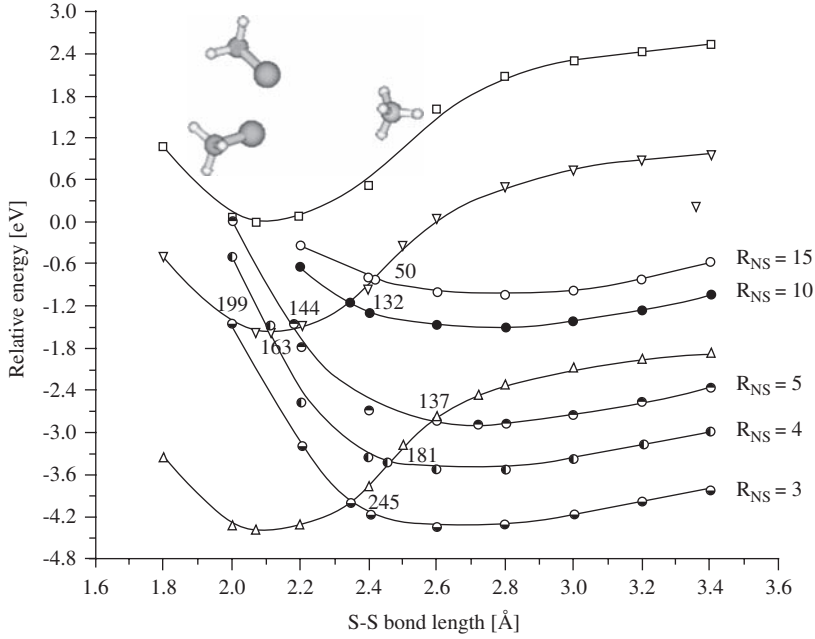

Figure 9 Energies of parent $H_3C-SS-CH_3 \ldots NH_4^+$ (open squares), ground-Rydberg (open triangles), excited-Rydberg (inverted open triangles), and various SS s*-attached (circles) states as functions of the SS bond length, for a range of distances between the nitrogen atom and the midpoint of the SS bond (appears in Figure 8 of ref. 3s).

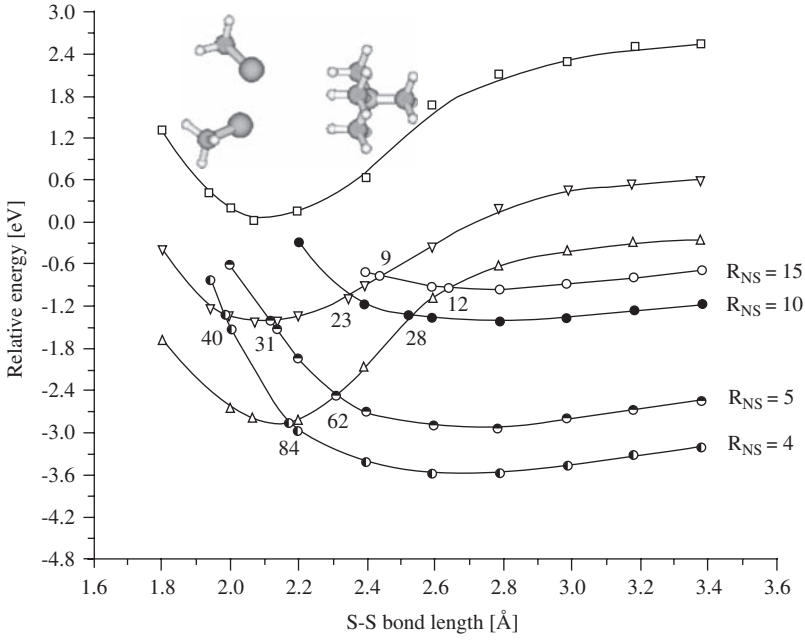

Figure 10 Energies of parent $H_3C-SS-CH_3 \ldots N(CH_3)_4^+$ (open squares), ground-Rydberg (open triangles), excited-Rydberg (inverted open triangles), and various SS s*-attached (circles) states as functions the SS bond length for a range of distances between the nitrogen atom and the midpoint of the SS bond (appears in Figure 8 of ref. 3s).

log of these $H_{1,2}$ values as functions of the distance from the nitrogen atom to the midpoint of the SS bond for the four cases related to Figures 9 and 10.

Again, we see that the Rydberg states' couplings can extend over very large distances. Moreover, it appears (from Figures 8 and 11) that the excited-Rydberg states' coupling strength seems to decay somewhat slower with distance than those of the ground-Rydberg states. Finally, the magnitudes of the $H_{1,2}$ values obtained with $-CH_2-$ spacers present are not qualitatively larger (compare Figures 8 and 11) than those obtained in the through-space study (for a given distance). This suggests that, at least for the systems studied to date, the presence of aliphatic spacers does not qualitatively increase the rates of intra-peptide electron transfer; through-space transfer seems to be dominant.

Although space limitations preclude reviewing all of the results [3h–3u] that have come out of our studies on anion-to-peptide electron transfer and intra-peptide electron transfer, it is worth mentioning here a few of the highlights.

a. In collisions of an anion donor with a positively charged polypeptide, electron transfer to a Rydberg orbital on a positive site is 10–100 times more likely than transfer to an SS σ* or OCN π* orbital.
b. Once an electron attaches to a Rydberg orbital (probably an excited orbital), it can relax to lower-energy Rydberg orbitals in *ca.* 1 μs, or it can, in this same timeframe, undergo transfer to any an SS σ* or OCN π* orbital that is within

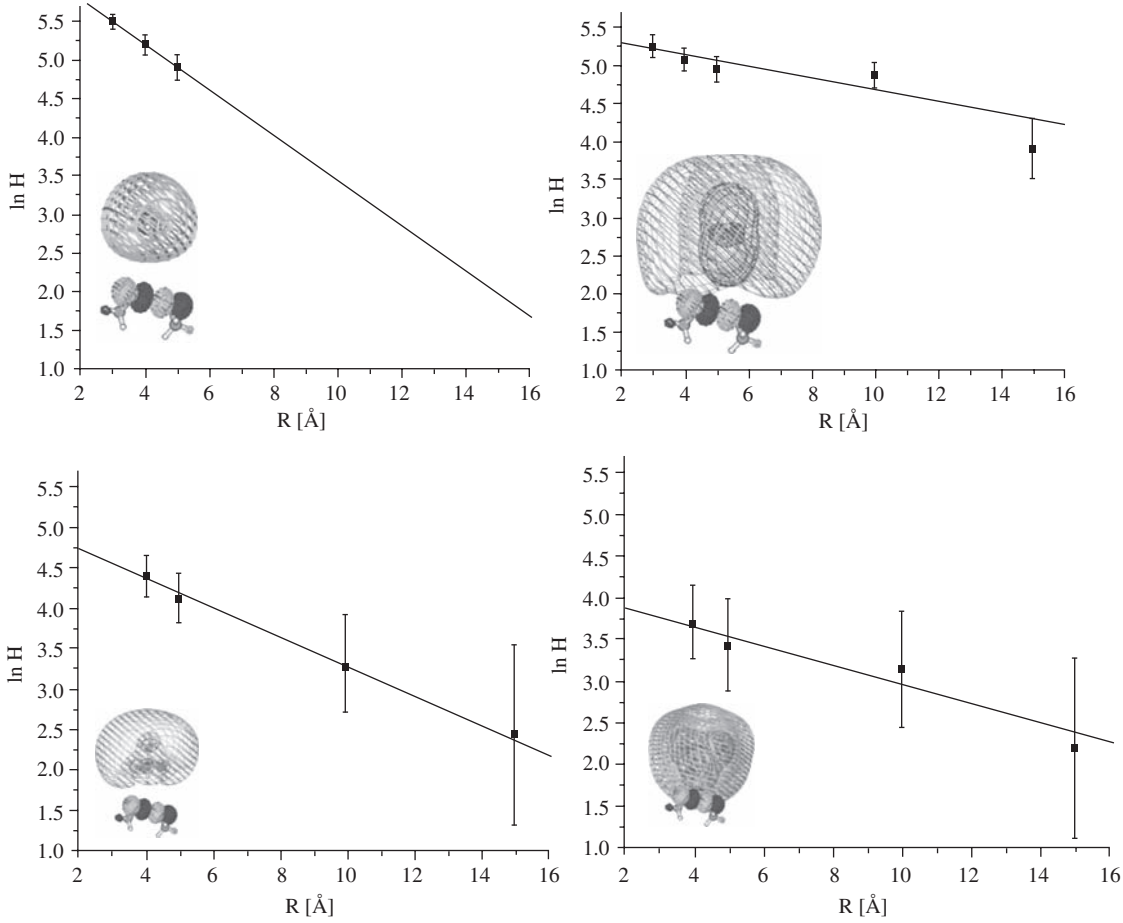

Figure 11 Plots of ln $H_{1,2}$ (cm^{-1}) vs. distance from the nitrogen atom to the midpoint of the SS bond for ground (left) and excited (right) Rydberg states of NH_4 (top) and $N(CH_3)_4$ (bottom). Also shown are the Rydberg orbitals involved in each case along with the molecular complex's geometry (appears as Figure 7 in ref. 3p).

15–20 Å and that is sufficiently Coulomb stabilized by nearby positive charges to render positive its electron binding energy.

c. Once an electron attaches to a Rydberg orbital, it can transfer to a Rydberg orbital on a different positive site if the two sites come within *ca.* 10 Å of each other.

3. RELATION TO MORE COMMON FORMS OF ELECTRON TRANSFER

Electron-transfer processes play many very important roles in chemistry and biology. Because the present work is focused on electron-transfer events occurring within positively charged gas-phase peptides as they occur in ETD and ECD mass spectrometry experiments, it is not appropriate or feasible to review the myriad of other places electron-transfer reactions occur in chemistry. Chapter 10 of the graduate level textbook by Schatz and Ratner [12] gives a nice introduction to the main kinds of electron-transfer events that chemists usually study as well as to the theoretical underpinnings. They also give, at the end of Chapter 10, several literature references to selected seminal papers on these subjects.

In most other electron-transfer processes, one considers an electron moving from a donor (D) to an acceptor (A) through an intervening molecular structure called a bridge (B). This is much like the Rydberg-bridge-SS system treated earlier in this paper. There are then two diabatic (meaning having a fixed orbital occupancy) electronic states D-B-A and D^+-B-A^- of the donor-bridge-acceptor system between which one views the transfer as taking place. The energy profiles of the reactant (D-B-A) and product (D^+-B-A^-) states as functions of a reaction coordinate X (i.e., the direction along which the two diabatic energy hypersurfaces cross) are, in the most commonly invoked theory, represented as parabolic functions whose minima are shifted in energy by $\varepsilon_2 - \varepsilon_1$ and in length along the reaction coordinate by $X_R - X_L$ as shown in Figure 12.

The two diabatic energy profiles are expressed in terms of harmonic forms having a common force constant as:

$$V_L(X) = \varepsilon_1 + \frac{1}{2}k(X - X_L)^2 \tag{4}$$

$$V_R(X) = \varepsilon_2 + \frac{1}{2}k(X - X_R)^2 \tag{5}$$

The two diabatic surfaces and wave functions are allowed to couple by way of a Hamiltonian matrix element denoted J:

$$J = \langle \psi_L | H | \psi_R \rangle \tag{6}$$

and two adiabatic energy surfaces are generated from the 2×2 Hamiltonian matrix

$$H = \begin{bmatrix} V_L & J \\ J & V_R \end{bmatrix} \tag{7}$$

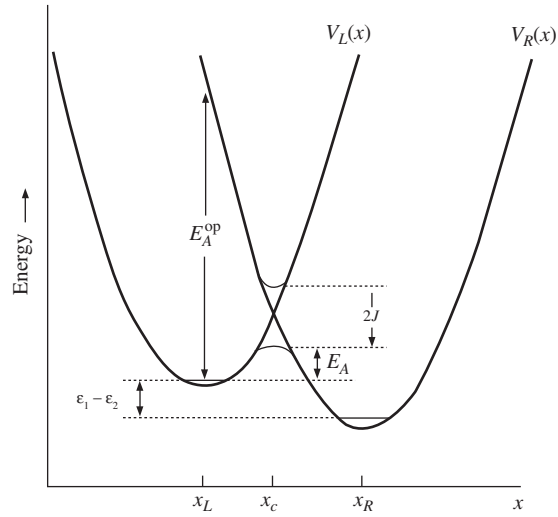

Figure 12 Plots of the energy surfaces appropriate to the D-B-A (left) and D^+-B-A^- (right) species as functions of the reaction coordinate along which the diabatic surfaces cross and the adiabatic surfaces undergo an avoided crossing (as shown) (appears as Figure 10.2 in ref. 12).

The two eigenvalues of this matrix

$$E_{\pm} = \frac{1}{2}[V_L + V_R \pm \sqrt{(V_R - V_L)^2 + 4J^2}] \tag{8}$$

differ by an amount $2J$ at the point X_C along the reaction coordinate at which the two diabatic curves cross (i.e., $V_L = V_R$ at X_C) as shown in Figure 12. The activation energy E_A (i.e., the energy needed to move from ε_1 to the barrier on the lower adiabatic energy surface (i.e., $E_-(X_C)$)) can be expressed in terms of the so-called reorganization energy Λ and the thermodynamic energy difference $\varepsilon_2 - \varepsilon_1$:

$$E_A = \frac{(\Lambda + \varepsilon_2 - \varepsilon_1)^2}{4\Lambda} \tag{9}$$

with

$$\Lambda = V_R(X_L) - V_R(X_R) \tag{10}$$

Λ is called the reorganization energy because (see Figure 12) it is the energy necessary to relax the system when it is in the D^+-B-A^- state but at the equilibrium geometry of the D-B-A state (having energy $V_R(X_L)$) to the energy of this D^+-B-A^- state at its own equilibrium geometry.

In the cases treated in the present paper, we do not have a reorganization energy because, for example as shown in Figures 5 and 10, the two diabatic states between which electron transfer occurs (e.g., the SS σ^* and excited-Rydberg states) cross so close (i.e., within the zero-point vibrational motion of the SS bond) to the minimum on the Rydberg-state surface as to render Λ essentially zero. In more traditional electron-transfer events, Λ contains contributions from the

energy needed to rearrange the geometry of the D-B-A molecule itself as well as the energy needed to relax the surrounding solvent environment to the change from D-B-A to D^+-B-A^-. That is, in D-B-A the surrounding solvent experiences a very different electrostatic potential than in D^+-B-A^-, so the solvent molecules must reorient (and polarize) to adjust to the change in this potential. However, as noted above, in our case, there is no intramolecular reorganization energy and no solvent contribution because the mass spectroscopy experiments are carried out in the gas phase.

Returning to the more common electron-transfer cases, as shown in ref. 12, the electron-transfer rate is eventually expressed as a product of two terms. One term, which depends on the activation energy E_A in the usual $\exp(-E_A/RT)$ manner contains the reorganization energy. The other term is proportional to J^2 and reflects the intrinsic electron-transfer rate once the system reaches the activation barrier. The scaling with J^2 arises when the couplings between the two diabatic states are treated perturbatively in this so-called nonadiabatic limit. In the cases treated in this paper, the electron-transfer rates depend on $H_{1,2}^2$ ($H_{1,2}$ is the same as J) through the LZ expression, but we have no $\exp(-E_A/RT)$ factor because, as already explained, our reorganization energies are essentially zero. They scale as $H_{1,2}^2$ because, in the LZ estimate of the surface hopping probability, the two diabatic states that cross are assumed to undergo a weakly avoided crossing; that is, the LZ estimate is in line with the nonadiabatic limit discussed in conventional electron-transfer theory.

Finally, it may be useful to note that the Fermi golden rule and time correlation function expressions often used (see ref. 12, for example) to express the rates of electron transfer have been shown [13], for other classes of dynamical processes, to be equivalent to LZ estimates of these same rates. So, it should not be surprising that our approach, in which we focus on events with no reorganization energy requirement and we use LZ theory to evaluate the intrinsic rates, is closely related to the more common approach used to treat electron transfer in condensed media where the reorganization energy plays a central role in determining the rates but the J^2 factor plays a second central role.

In closing, it may be instructive to contrast the electron-transfer events taking place in polypeptides with those we have been studying relating to electrons in DNA [14]. In these studies, we simulate processes in which

a. an electron attaches to a π^* orbital on one of DNA's bases, after which
b. the electron can autodetach, or
c. it can undergo a transfer through the sugar unit attached to the base and into the sugar-phosphate C–O σ bond's antibonding orbital, thus leading to C–O bond cleavage and a so-called single strand break.

The branching ratio between autodetachment and electron transfer governs the yield of strand breaks. In Figure 13, we show a qualitative depiction of the energy surfaces involved in this class of electron-transfer processes.

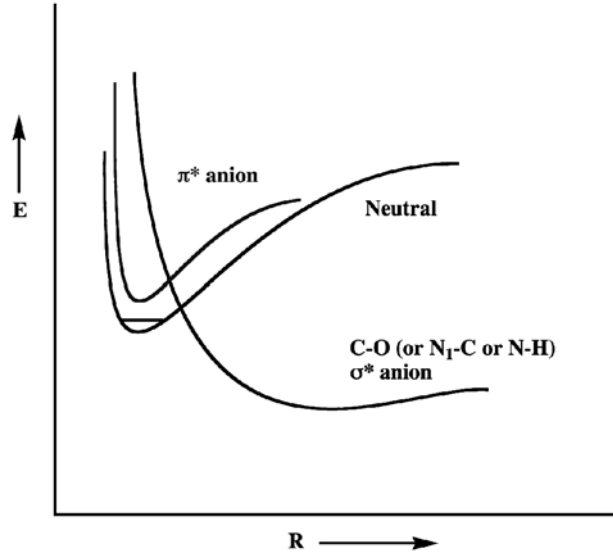

Figure 13 Qualitative depiction, as functions of the sugar-phosphate C–O bond length, of the energy of a base-sugar-phosphate nucleotide with no electron attached (labeled neutral), with an electron attached to its base π* orbital (labeled π* anion), and with the electron residing in the sugar-phosphate C–O σ* orbital (lower curve) (appears as Figure 7 in ref. 14).

There are two primary differences in this DNA case when compared to the polypeptide systems discussed earlier:

1. Because the repulsive C–O σ*-attached state crosses the base π*-attached state at an energy significantly above the minimum on the π*-attached state's surface (see Figure 13), the C–O bond must undergo substantial elongation to access this crossing point. This elongation is thought to occur by thermal excitation of the C–O stretching motion. The energy ΔE required to reach this crossing is analogous to the reorganization energy discussed earlier. This requirement gives rise to a Boltzmann $\exp(-\Delta E/RT)$ dependence in the electron-transfer rate for this DNA case, much like the reorganization energy does in the conventional electron-transfer theory discussed earlier.
2. The $H_{1,2}$ matrix elements connecting the C–O σ*-attached and the base π*-attached states were found [14] to be much larger (e.g., $>1{,}000\,\mathrm{cm}^{-1}$) than in the polypeptide case (where they were usually $<300\,\mathrm{cm}^{-1}$). As a result, the DNA electron transfer does not occur in the nonadiabatic limit discussed earlier as it does in the polypeptides. In the DNA case, the couplings are large enough that the system evolves adiabatically (i.e., once the barrier at the crossing of the C–O σ*-attached and the base π*-attached states is reached, electron transfer is prompt) from the base to the sugar-phosphate C–O bond that is then cleaved.

ACKNOWLEDGMENT

This work has been supported by NSF Grant No. 0806160.

REFERENCES

1. [a] Zubarev, R.A., Kelleher, N.L., McLafferty, F.W. Electron capture dissociation of multiply charged protein cations. A nonergodic process. J. Am. Chem. Soc. 1998, 120, 3265–6. [b] Zubarev, R.A., Kruger, N.A., Fridriksson, E.K., Lewis, M.A., Horn, D.M., Carpenter, B.K., McLafferty, F.W. Electron capture dissociation of gaseous multiply-charged proteins is favored at disulfide bonds and other sites of high hydrogen atom affinity. J. Am. Chem. Soc. 1999, 121, 2857–62. [c] Zubarev, R.A., Horn, D.M., Fridriksson, E.K., Kelleher, N.L., Kruger, N.A., Lewis, M.A., Carpenter, B.K., McLafferty, F.W. Electron capture dissociation for structural characterization of multiply charged protein cations. Anal. Chem. 2000, 72, 563–73. [d] Zubarev, R.A., Haselmann, K.F., Budnik, B., Kjeldsen, F., Jensen, F. Account: towards an understanding of the mechanism of electron-capture dissociation: a historical perspective and modern ideas. Eur. J. Mass Spectrom. 2002, 8, 337–49.
2. [a] Syka, J.E.P., Coon, J.J., Schroeder, M.J., Shabanowitz, J., Hunt, D.F. A bubble-driven microfluidic transport element for bioengineering. Proc. Natl. Acad. Sci. 2004, 101, 9523–8. [b] Coon, J.J., Syka, J.E.P., Schwartz, J.C., Shabanowitz, J., Hunt, D.F. Anion dependence in the partitioning between proton and electron transfer in ion/ion reactions. Int. J. Mass Spectrom. 2004, 236, 33–42. [c] Pitteri, S.J., Chrisman, P.A., McLuckey, S.A. Electron-transfer ion/ion reactions of doubly protonated peptides: effect of elevated bath gas temperature. Anal. Chem. 2005, 77, 5662–9. [d] Gunawardena, H.P., He, M., Chrisman, P.A., Pitteri, S.J., Hogan, J.M., Hodges, B.D.M., McLuckey, S.A. Electron transfer versus proton transfer in gas-phase ion/ion reactions of polyprotonated peptides. J. Am. Chem. Soc. 2005, 127, 12627–39. [e] Gunawardena, H.P., Gorenstein, L., Erickson, D.E., Xia, Y., McLuckey, S.A. Electron transfer dissociation of multiply protonated and fixed charge disulfide linked polypeptides. Int. J. Mass Spectrom. 2007, 265, 130–8.
3. [a] Syrstad, E.A., Turecek, F. Hydrogen atom adducts to the amide bond. Generation and energetics of the amino(hydroxy)methyl radical in the gas phase. J. Phys. Chem. A 2001, 105, 11144–55. [b] Turecek, F., Syrstad, E.A. Mechanism and energetics of intramolecular hydrogen transfer in amide and peptide radicals and cation-radicals. J. Am. Chem. Soc. 2003, 125, 3353–69. [c] Turecek, F., Polasek, M., Frank, A., Sadilek, M. Transient hydrogen atom adducts to disulfides. Formation and energetics. J. Am. Chem. Soc. 2000, 122, 2361–70. [d] Syrstad, E.A., Stephens, D.D., Turecek, F. Hydrogen atom adducts to the amide bond. Generation and energetics of amide radicals in the gas phase. J. Phys. Chem. A 2003, 107, 115–26. [e] Turecek, F. NCα bond dissociation energies and kinetics in amide and peptide radicals. Is the dissociation a non-ergodic process? J. Am. Chem. Soc. 2003, 125, 5954–63. [f] Syrstad, E.A., Turecek, F. Toward a general mechanism of electron capture dissociation. J. Am. Soc. Mass. Spectrom. 2005, 16, 208–24. [g] Uggerud, E. Electron capture dissociation of the disulfide bond—a quantum chemical model study. Int. J. Mass Spectrom. 2004, 234, 45–50. [h] Anusiewicz, I., Berdys-Kochanska, J., Simons, J. Electron attachment step in electron capture dissociation (ECD) and electron transfer dissociation (ETD). J. Phys. Chem. A 2005, 109, 5801–13. [i] Anusiewicz, I., Berdys-Kochanska, J., Skurski, P., Simons, J. Simulating electron transfer attachment to a positively charged model peptide. J. Phys. Chem. A 2006, 110, 1261–6. [j] Sawicka, A., Skurski, P., Hudgins, R.R., Simons, J. Model calculations relevant to disulfide bond cleavage via electron capture influenced by positively charged groups. J. Phys. Chem. B 2003, 107, 13505–11. [k] Sobczyk, M., Skurski, P., Simons, J. Dissociative low-energy electron attachment to the C–S bond of H_3C-SCH_3 influenced by Coulomb stabilization. Adv. Quantum Chem. 2005, 48, 239–51. [l] Sawicka, A., Berdys-Kochaska, J., Skurski, P., Simons, J. Low-energy (0.1 eV) electron attachment S–S bond cleavage assisted by Coulomb stabilization. Int. J. Quantum Chem. 2005, 102, 838–46. [m] Anusiewicz, I., Berdys, J., Sobczyk, M., Sawicka, A., Skurski, P., Simons, J. Coulomb-assisted dissociative electron attachment: application to a model peptide. J. Phys. Chem. A 2005, 109, 250–8. [n] Bakken, V., Helgaker, T., Uggerud, E. Models of fragmentations induced by electron attachment to protonated peptides. Eur. J. Mass Spectrom.

2004, 10, 625–38. [o] Skurski, P., Sobczyk, M., Jakowski, J., Simons, J. Possible mechanisms for protecting N–Ca bonds in helical peptides from electron-captue (or transfer) dissociation. Int. J. Mass Spectrom. 2007, 265, 197–212. [p] Sobczyk, M., Neff, D., Simons, J. Theoretical study of through-space and through-bond electron transfer within positively charged peptides in the gas phase. Int. J. Mass Spectrom. 2008, 269, 149–64. [q] Sobczyk, M., Simons, J. Distance dependence of through-bond electron transfer rates in electron-capture and electron-transfer dissociation. Int. J. Mass Spectrom. 2006, 253, 274–80. [r] Sobczyk, M., Simons, J. The role of excited Rydberg states in electron transfer dissociation. J. Phys. Chem. B 2006, 110, 7519–27. [s] Neff, D., Sobczyk, M., Simons, J. Through-space and through-bond electron transfer within positively charged peptides in the gas phase. Int. J. Mass Spectrom. 2008, 276, 91–101. [t] Neff, D., Simons, J. Theoretical study of electron capture dissociation of $[Mg(H_2O)_n]^{2+}$ clusters. Int. J. Mass Spectrom. 2008, 277, 166–74. [u] Simons, J. Molecular anions. J. Phys. Chem. A 2008, 112, 6401–511. [v] Neff, D., Smuczynska, S., Simons, J. Electron shuttling in electron transfer dissociation. Inter. J. Mass Spec. 2009, 283, 122–34. [w] Neff, D., Simons, J. Analytical and computational studies of intra-molecular electron transfer pertinent to electron transfer and electron capture dissociation mass spectrometry. J. Phys. Chem. A (submitted, 2009).

4. Gutowski, M., Simons, J. Lifetimes of electronically metastable double-Rydberg anions: FH_2^-. J. Chem. Phys. 1990, 93, 3874–80.
5. Simons, J., Gutowski, M. Double-Rydberg molecular anions. Chem. Rev. 1991, 91, 669–77.
6. Skurski, P., Gutowski, M., Simons, J. How to choose a one-electron basis set to reliably describe a dipole-bound anion. Int. J. Quantum Chem. 2000, 80, 1024–38.
7. Pauling, L., Wilson, E.B. Jr. Introduction to Quantum Mechanics with Applications to Chemistry, Dover Publications, New York, 1985.
8. McConnell, H.M. Intramolecular charge transfer in aromatic free radicals. J. Chem. Phys. 1961, 35, 508.
9. Mujica, V., Kemp, M., Ratner, M.A. Electron conduction in molecular wires. II. Application to scanning tunneling microscopy. J. Chem. Phys. 1994, 101, 6856.
10. Jordan, K.D., Paddon-Row, M.N. Long-range interactions in a series of rigid nonconjugated dienes. 1. Distance dependence of the π_+, π_- and π^*_+, π^*_- splittings determined by ab initio calculations. J. Phys. Chem. 1992, 96, 1188.
11. Curtiss, L.A., Naleway, C.A., Miller, J.R. Superexchange pathway calculation of long-distance electronic coupling in $H_2C(CH_2)_{m-2}CH_2$ chains. Chem. Phys. 1993, 176, 387.
12. Schatz, G.C., Ratner, M.A. Quantum Mechanics in Chemistry, Prentice Hall, Englewood Cliffs, NJ, 1993.
13. Taylor, H., Simons, J. A different view of molecular electronic transitions. J. Phys. Chem. 1986, 90, 580–3.
14. Simons, J. How do low-energy (0.1−2 eV) electrons cause DNA strand breaks? Acc. Chem. Res. 2006, 39, 772–9.

SUBJECT INDEX

CUMULATIVE INDEX VOLS 1–5